A Network of Networks to Reproduce the Electrical Features of an Aptamer-ligand Complex

What an Electrical Network Tells about Affinity

Eleonora Alfinito[1], Rosella Cataldo[2] and Lino Reggiani[2]

[1]Dipartimento di Ingegneria dell'Innovazione, Salento University, Lecce, Italy
[2]Dipartiemnto di Matematica e Fisica "Ennio de Giorgi", Salento University, Lecce, Italy

Keywords: Networks, Proteotronics, Aptamers, Aptasensors.

Abstract: The increasing interest in the production and selection of aptamers for therapeutic and diagnostic applications yields many studies in recent years. Most of them investigated the production techniques, usually performed *in vitro,* but also the possibility of an *in silico* selection. Due to their specific ability of target-inhibition, some aptamers are under clinical trials, and some other were just patented by several pharmaceutical companies. However, the mechanism of aptamer-ligand formation is not completely understood. In this paper we explore the possibility to describe some topological and electrical features of the aptamer TBA alone and complexed with thrombin, its specific ligand, by using a network consisting of two different networks. The results are quite intriguing, confirming some conjectures about the different role of two cations, i.e. Na^+ and K^+, in stabilizing the compound. Furthermore, this study suggests the use of resistance measurements to discriminate among different affinities.

1 INTRODUCTION

The current trend in medicine is the improvement of prevention (vaccination, disease screening, correct lifestyle, etc.), the personalization of treatments and a less invasive and friendly (for example, point-of-care) diagnostics. Accordingly, the development of new techniques and therapies is widely explored. Outstanding results are given by aptamers, which are small fragments of ssDNA or RNA, artificially produced to perfectly adapt to an assigned ligand (from small molecules to large proteins).

The selection and amplification technique used to produce aptamers is called SELEX (Systematic Evolution of Ligands by EXponential Enrichment) (Oliphant, 1989, Ellington, 1990, Tuerk, 1990). This technique seems so powerful to produce, in principle, an aptamer for each specific pathogen or macromolecule found at the origin of a disease. It could be a revolution in medicine.

In the last 20 years, big efforts have been devoted to the production of even more efficient aptamers, by using both biochemical and computational techniques (Yüce, 2015, Jo, 2016). Some of them are at the first/second stage of clinical trials, and this result gives hope of a more and more massive use in medicine (Ni, 2011).

The mechanism of ligand binding has been compared to the structural recognition process used by antibodies to capture antigens, therefore aptamers are also known as "chemical antibodies" (Sun, 2014). Like antibodies, they bind the target with high specificity and selectivity and, therefore, this has awakened a wide interest for the possible technological uses. As a consequence, a rapid development of aptasensors, i.e. sensors based on aptamers (Iliuk, 2011) has taken place. Indeed, aptamers are used in biosensors in substitution of antibodies, which are, usually, more difficult to produce and often require animal sacrifice. Despite all the progresses made in the field of aptamer production and selection, so as in the aptamer technological and medical applications, the understanding of the biochemical and physical processes underling the aptamer/protein-ligand interaction is still quite poor (Du, 2016).

In this paper we focus attention on the small 15-mer TBA (5'-GGT TGG TGT GGT TGG-3`), whose ability in the inhibition of the enzyme thrombin is well known. Thrombin is an enzyme present in

mammals blood where rules coagulation. Therefore, in some diseases, like heart attack, its inhibition is part of the therapy. TBA passed the first step of the clinical trials; at present, a modified version of this aptamer, which ensures a longer permanence in human body, has been patented and is currently used in clinics.

Recently, TBA has been successfully used in a prototype of thrombin sensor (Cai, 2005). This device is sensitive to thrombin in a range of 6 orders of magnitude and selective with respect non-thrombin molecules. Furthermore, the detection technique, based on electrochemical impedance spectroscopy, is well consolidated. At present, the only -although quite serious- constraint to its large scale diffusion is miniaturization, which should allow for point-of-care uses.

The aim of this paper is to show that a network of networks can be a good tool for investigating some electrical properties of the complex TBA-thrombin, each of them represented by a specific network. Specifically, this tool, which is contained in a more wide approach called proteotronics (Alfinito, 2015), is able to correctly describe and interpret some relevant results obtained by using X-ray spectrometry (Russo–Krauss, 2012), and electrochemical impedance spectroscopy (EIS) measurements (Cai, 2005). In particular, this approach is able to foresee the reduced affinity of the TBA-thrombin composite, when produced in the presence of Na^+, with respect to that of the same compound, produced in a solution containing K^+. Furthermore, the resistance variation observed in EIS measurement is also well reproduced. Finally, the results reveal a very interesting feature: the protein binding lowers instead of increasing the aptamer resistance. As a matter of fact, compared to the aptamer in the native state, there is an increase of resistance, in agreement with experiments, but, compared to the aptamer in the active state, the resistance decreases. This is an unexpected result, which is mainly related to the complex structure of the associated interconnected networks.

2 MATERIALS AND METHODS

The network of networks is built up starting from the single networks representing the protein and the aptamer, respectively. In particular, to build up the networks we use:
  a. the aptamer in its native state, i.e. its lowest free energy state;

  b. The aptamer in its active form, i.e. the aptamer with the structure deformed due to the binding but deprived of the protein, in the presence of both K^+ and Na^+;
  c. The aptamer-enzyme complex, in the presence of both K^+ and Na^+;
  d. The enzyme alone in the presence of both K^+ and Na^+.

Structure a. is available from the Protein Data Bank (Berman, 2000) at the entry 148D (Schultze, 1994), while structures b-d are available from the Protein Data Bank at the entries: 4DII and 4DIH (Russo-Krauss, 2012).

Furthermore, each network has been equipped with specific electrical features and can be used to explore the topological and electrical properties of the corresponding biomolecule. The complete network, the network of networks, is obtained by using the 3D structure of the complex aptamer-thrombin and allowing appropriate electrical interactions between the different macromolecules, as described in Section 2.2

2.1 Topological Methods

Each structure is mapped into a complex network whose nodes correspond to the position of the C_1 carbon atoms, for the aptamer, and to that of the C_α carbon atoms for the enzyme. The nodes are connected with a simple cut-off rule, i.e. only if the distance is smaller than an assigned value, R_C.

In such a way, some topological features, like the structure deformation subsequent to the protein attachment, can be easily described. Figure 1 shows the adjacency matrix, also known as contact map (each point represents the link between the nodes corresponding to the point coordinates) of the aptamer in the active form, in the presence of Na^+ and K^+. The value of the interaction radius is 10Å.
The contact maps are equal. Nevertheless, the aptamer-thrombin complex shows tiny differences in the structure when produced in the presence of the two different cations, see Figure 2.

In brief, these results tell us that the cations slightly affect the topological structure of the complex. Anyway, it is well known that affinity does depend on the solvent (Russo-Krauss, 2012), therefore we proceed with a more detailed investigation.
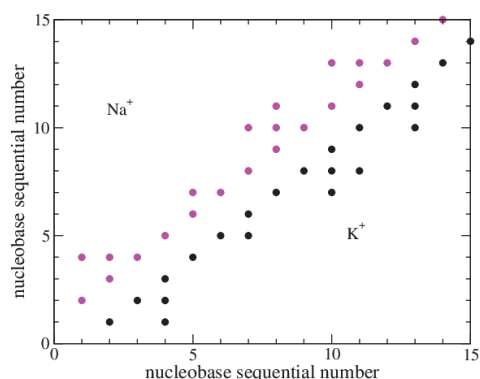
Figure 1: Contact map of TBA in the active state, in solution with two different cations, Na^+, magenta, and K^+, black (color online).
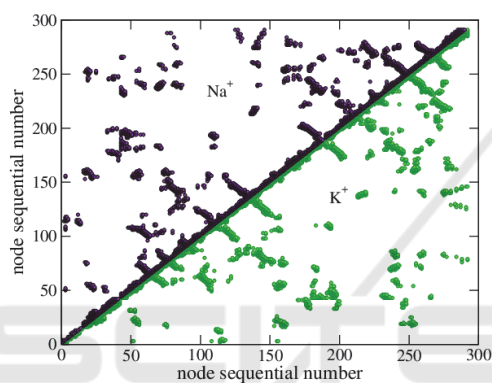

Figure 2: Contact map of the complex TBA-thrombin in solution with two different cations, Na^+, black, and K^+, green (color online).

Complementary information concerning the network structure is given by the degree distribution. Figure 3 reports the degree distribution of the TBA in the native structure and active state, $R_C=10$Å.
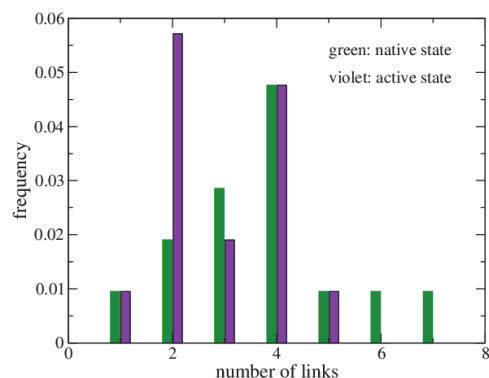

Figure 3. Degree distribution of TBA in the native and active state, $R_C=10$Å. The degree distribution of the active state does not depend on the ion in solution (color online).

The degree distribution of the native state has a typical Poisson-like shape. The degree distribution of the active state does not depend on the kind of ions used in the solution; the maximum has shifted at the value 2, and there are not more nodes with more 5 links. This means that the structure is more dilated than the native one.

On the other hand, when we give a look to the degree distribution of the enzyme alone (Figure 4, full histograms), we notice small but noticeable differences depending on the used ions.
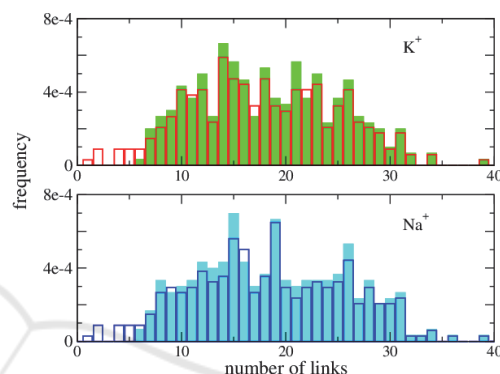

Figure 4: Degree distribution of the TBA-thrombin complex, $R_C=10$Å (empty histogram) and the thrombin alone (full histogram).

As expected, in the TBA-thrombin complex (empty histograms) the number of nodes with a small number of links is larger (due to the dilated structure of the aptamer).

The structure resolved in the solution containing potassium has a Poisson-like degree distribution, while the structure resolved in a solution containing sodium is more flat. A more detailed investigation on this topic is in progress.

In conclusion, the topological analysis reveals that the differences between the macromolecules in the presence of the cations K^+ and Na^+ are quite subtle and mainly concern the degree distribution. These differences are amplified by the electrical response, as described in the following section.

2.2 Electrical Methods

To investigate the electrical response of the macromolecules we built up the corresponding electrical network.

The single protein electrical network is produced as in previous investigations (Alfinito, 2009, Alfinito, 2010). In particular, each link is thought as an electrical line with a specific resistance and

capacitance. Each passive element of this line is geometrically represented by a cylinder of height l, the distance between the nodes, and basis area A, the intersection area of two spheres of radius R_C centred in each of the nodes. The resulting electrical impedance depends on the kind of nodes (here amino acids or nucleobases) and on their distance. Finally, the impedance of the link between the nodes a,b writes:

$$Z_{a,b} = \frac{l_{a,b}}{A_{a,b}} \frac{\rho_{a,b}}{1+i\varrho\varepsilon_0\varepsilon_{a,b}\omega} \qquad (1)$$

where $\rho_{a,b}$ and $\varepsilon_{a,b}$ are the resistivity and the dielectric constant of the link, ω is the frequency of the applied voltage. The polarizability values are quite different for amino acids and nucleic bases (and, in principle, also the macroscopic electric response of aptamers could be not the same observed in proteins (Akimov, 2008)). Here we assume that, in similar experimental conditions, aptamers and proteins have similar electrical behaviors and formulate our model accordingly.

The aptamer electrical features are modelled by using the values of resistivity and polarizability of the AGCTU set, recently published (Ohshiro, 2012, Šponer, 2001). Specifically, the relative dielectric constant of the couple of the a-th and b-th nodes, $\varepsilon_{a,b}$, is expressed in terms of the intrinsic polarizability of each isolated amino acid/nucleobase, α_{elec} (Šponer, 2001), and writes:

$$\varepsilon_{a,b} = 1 + \frac{4\pi\left(\alpha_{elect,a}+\alpha_{elect,b}\right)}{6} \qquad (2)$$

where the second term in the r.h.s. describes the mean value of the polarizability of the couple of nodes.

The resistivities of the nucleobases are taken by (Ohshiro, 2012), $\rho_a = \overline{\rho}\delta_a$, where $\overline{\rho}$ is the mean value calculated upon the AGCTU set and δ is the fraction $\rho/\overline{\rho}$ for each nucleobase. Therefore, the resistivity of the link drawn between the a-th and the b-th nucleobase is defined as :

$$\rho^N_{a,b} = \frac{\overline{\rho}\left(\delta_a+\delta_b\right)}{2} \qquad (3)$$

Since analogous data are not given for amino acids, for the sake of simplicity, we assume that their resistivities are all the same. In particular, the link resistance of a couple of amino acids is:

$$\rho^A_{a,b} = \overline{\rho} \quad . \qquad (4)$$

The region between the networks, where the hooking happens, is the most interesting. Here the protein perfectly matches the aptamer and combines with it *via* van der Waals forces. It has been revealed that the presence of some ions like Na^+ and K^+ gives TBA a different ability to inhibit thrombin (Russo-Krauss, 2012). Furthermore, in previous sections we have seen that these cations poorly affect the TBA-enzyme structure.

Accordingly, we conjecture that most of these differences are due to the small interaction region. Therefore, we assume that previous formulas still hold in each part of the network of networks. This is also true in the aptamer-thrombin contact region, but with features intermediate between those of amino acids and nucleobases. In particular, for the couple of the a-th nucleobase and b-th amino acid, the link resistance is:

$$\rho^{NA}_{a,b} = \frac{\overline{\rho}\left(\delta_a+1\right)}{2} \quad . \qquad (5)$$

Equation (2) is modified accordingly.

Each electrical network is ideally contacted to an external bias, by using the first and the last node as terminals. The electrical features of this linear network are calculated by using the Kirchhoff laws, applied to a set of linear equations. Finally, the equations are numerically solved by a standard computational procedure which has its roots in the so-called random resistor network method (De Arcangelis, 1985, Pennetta, 2004) and has driven to the proteotronic approach (Alfinito, 2015, Alfinito, 2009).

2.3 Thrombin Inhibition - the Energy Funnel Framework

The exact mechanism of thrombin inhibition is, at present, quite unclear and, in general, the protein activation due to a specific ligand is a long time debated problem (Onuchic, 1994, Kobilka, 2007). Here we describe the process of TBA-thrombin conjugation from the point of view of the energy transitions the single macromolecule and the compound perform (Alfinito, 2017, Alfinito, 2016). First of all, when the protein/aptamer assumes its native and stable configuration, its energy is on the bottom of a configurational energy funnel (the native funnel) which corresponds to the set of energies the macromolecule has when it goes from the molten to

the native state. When it receives energy from the environment it can go up in the funnel. A way to receive energy is to be surrounded by the specific ligands. The ligands can smoothly improve the aptamer energy simply striking it. Otherwise, when they bind the aptamers, they produce a sharp energy jump into a different funnel, the bond funnel. As a final result, the macromolecule changes its conformation and binds the ligand. Therefore, the energy funnel changes (binding funnel). In conclusion, the addition of specific ligands produces both the shift of energy in the native funnel and the transition to the binding energy funnel. A cartoon describing these two mechanisms is given in Figure 5. This complex mechanism is described, inside the impedance network analogue, with a change of the value of R_C (Alfinito, 2017, Alfinito, 2016). In doing so, we follow the model proposed by Kobilka and Deupi (Kobilka, 2007) which describes the protein dynamics in a process of binding as a transition between a couple of energy funnels. Furthermore, this induces a change of the number of internal bonds, preserving only those useful for stabilizing the final configuration.
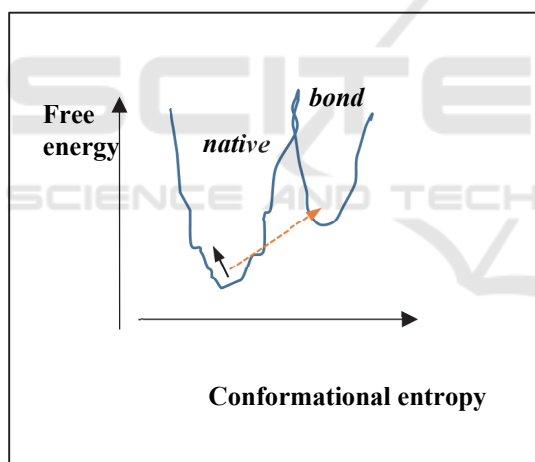

Figure 5: Sketch of the two possible energy transformations between two contiguous energy funnels, due to the aptmer-ligand interaction. Continuous line represents a smooth transition and dashed line an abrupt transition.

3 THEORY AND EXPERIMENTS

In this section we compare some experimental data concerning the structural and inhibitory properties of TBA with theoretical data coming from our model.

3.1 Resistance Data

It is well known that ions play an important role in stabilizing the 3D structure of TBA, the so-called G-quadruplex. In particular, by adding K^+ ions, the result is a more stable G-quadruplex and an increased inhibitory activity of thrombin (Russo- Krauss, 2012) .

The resistance spectra produced within the proteotronic approach are represented in Figure (6). In particular, in Figure 6a, the resistance of TBA activated in the presence of K^+ and Na^+ is reported in comparison with the resistance of TBA in the native state, for different values of R_C. Activation produces a resistance increase mainly in the region 8-16 Å. The main difference is obtained for $R_C=10$Å and is the same for both the activated structures.
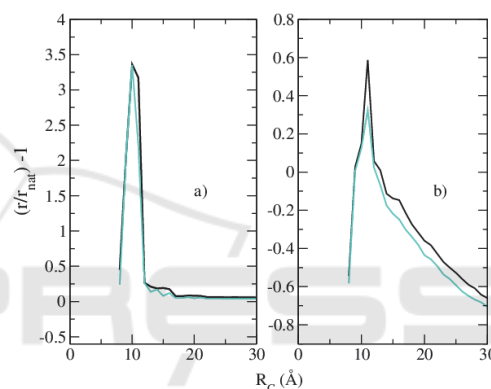

Figure 6. Relative resistance variation of TBA in the active state (a), or complexed with thrombin (b), vs. TBA in the native state. Turquoise lines refer to structures in the presence of K^+, black lines refer to structures in the presence of Na^+ (color online).

On the other hand, when the protein is added, Figure 6b, the resistance variation becomes strongly depend on the kind of ions in solution. Furthermore, it is quite smaller than that observed for the activated structures (notice the different scales in Figures (6a) and (6b)). Therefore, the protein does not produce a simple passivation, but it integrates the network of the TBA in the active state and globally reduces its resistance.

The TBA-thrombin structure obtained in the presence of K^+ has a larger resistance compared to the same structure obtained in the presence of Na^+, more close to that observed in experiments. This prompt us to explore this structure for further investigations.

3.2 EIS Data: Experiment

The experimental outcomes we refer for testing our model concern with the use of TBA in an electrochemical impedance spectroscopy assay (Cai, 2005).

In particular, a gold electrode, functionalized with TBA, was used to perform electrochemical measurements in the absence of thrombin and after incubation with different concentrations of the enzyme (from to 1 pM to 1 μM). The increasing protein concentration produced an increase of the electron transfer resistance, sufficient to fairly resolve different concentrations (a variation larger than 150 % for the highest concentration was measured).
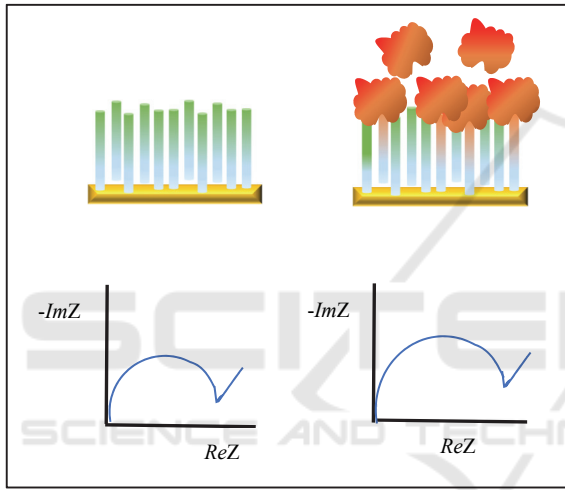
A sketch of the experiment is shown in Figure 7.

Figure 7. Schematic view of the experiment by Cai and co-workers. On top, the gold electrode functionalized with TBA without (left) and with (right) thrombin. On bottom the EIS response, with a sensitive variation of impedance due to thrombin.

3.3 EIS Measurements: Theory

Our model describes the behaviour of a single macromolecule, therefore, to compare our data with experiments, it is necessary to perform a rescaling. In particular, we are interested in the comparison of resistance data and it is made by using the following formula (Alfinito, 2017):

$$r_{sample} = N \cdot [f \times r_{com} + (1-f) \times r_{nat}] \quad (6)$$

where r_{sample} is the sample resistance, r_{com} the resistance of a single TBA-thrombin complex, and r_{nat} the resistance of the single TBA in the native state. N is the total number of aptamers on the electrode and f is the fraction of them bound to the protein. We

estimate the f value by assuming it is described by the Hill-like equation:

$$f = \frac{x^a}{b + x^a} \quad (7)$$

where $x = (R_0 - R_C)/R_0$, R_0 is the value of R_C corresponding to $f=0$ i.e. a sample consisting only of TBAs in their native state, and a and b are numerical fitting parameters. Equation (7) states a functional dependence between f and the value of the interaction radius, in agreement with Sec.2.3.

In the present case, we assume R_0=13.3Å, which is the value corresponding to zero difference between the resistance of the aptamer alone and that of the complete macromolecule. Furthermore, this value is the largest corresponding to the region in which, in agreement with experiments, the resistance of the complex TBA-thrombin is larger than that of the TBA in the native state (see Figure 6). By simultaneously using Equations (6,7) we are able to reproduce the experimental data. In particular, by using in Equation (7) the fitting parameters, a=2.99 and b=2.7 10^{-4}, Equation (6) reproduces the sample resistance variation observed by Cai and coworkers.

The results are given in Table 1.

Table 1: The rate r/r_0 of the sample electron-transfer resistance, R_{et}, measured for different thrombin concentrations with respect the sample R_{et} without thrombin; the corresponding theoretical quantities calculated for the values of R_C shown in column 3, and the fraction, f, of aptamer-thrombin complex.

r/r_0 experiment	r/r_0 theory	R_C (Å)	f
2.6±0.6	3.2	11.3	0.93
2.2±0.5	2.1	11.5	0.90
2.2±0.7	1.8	11.7	0.87
1.7±0.5	1.2	12.7	0.26

4 CONCLUSIONS

We have used a network of networks for analysing the electrical features of the complex constituted by the aptamer TBA and its specific ligand, the enzyme thrombin. The inhibition activity of TBA on this protein is a long time known result, also investigated to produce a targeted therapy with reduced side

effects. Furthermore, it has been also considered for producing a thrombin biosensor.

We have adapted a procedure previously used for a single protein to the aptamer alone, complexed with the specific ligand, and also without the ligand but with the modified structure it assumes when binds the ligand. The aptamer structures, taken by the Protein Data Bank, describe the oligomers in two different solutions. We observe that the electrical responses of the corresponding networks do not depend on the kind of solution (with Na^+ or K^+), for the case of the aptamer alone. On the other hand, when the protein binds the aptamer, the different action of the two cations is reflected by a different resistance response. Thus, this definitely confirms the relevant role of the cations in the binding mechanism. In other words, the cation steric action determines the shape of the network, and finally, the inhibition activity of TBA. In a more pragmatic approach this results suggest that a measure of resistance could be a test of affinity.

Another important result obtained with the technique of the network of networks is that by adding a large protein like the thrombin to TBA in its active form, the global resistance is lower than that of the aptamer. This is an important information concerning the mechanism of binding because it reveals that the protein efficaciously completes the not trivial structure of the aptamer, producing a global improvement of its conductance. Of course, and in agreement with experiments, the final resistance value is lower than that of the aptamer in the native state, but larger than that of the aptamer in the active state.

This enforces the conclusion that, at this level of microscopic interactions, the bulk approximation fails.

REFERENCES

Akimov, V., Alfinito, E., Bausells, J., Benilova, I., Paramo, I.C., Errachid, A., Ferrari, G., Fumagalli, L., Gomila, G., Grosclaude, J. and Hou, Y., 2008. Nanobiosensors based on individual olfactory receptors. *Analog Integrated Circuits and Signal Processing*, *57*(3), pp.197-203.

Alfinito, E., Pennetta, C. and Reggiani, L., 2009. Topological change and impedance spectrum of rat olfactory receptor I7: A comparative analysis with bovine rhodopsin and bacteriorhodopsin. *Journal of Applied Physics*, *105*(8), p.084703.

Alfinito, E., Pennetta, C. and Reggiani, L., 2010. Olfactory receptor-based smell nanobiosensors: an overview of theoretical and experimental results. *Sensors and Actuators B: Chemical*, *146*(2), pp.554-558.

Alfinito E., Pousset J., and Reggiani L.,2015 *Proteotronics: Development of Protein-Based Electronics*. CRC Press.

Alfinito, E. and Reggiani, L., 2016. Current-voltage characteristics of seven-helix proteins from a cubic array of amino acids. *Physical Review E*, *93*(6), p.062401.

Alfinito, E., Reggiani, L., Cataldo, R., De Nunzio, G., Giotta, L. and Guascito, M.R., 2017. Modeling the microscopic electrical properties of thrombin binding aptamer (TBA) for label-free biosensors. *Nanotechnology*, *28*(6), p.065502.

Berman, H.M., Westbrook, J., Feng, Z., Gilliland, G., Bhat, T.N., Weissig, H., Shindyalov, I.N. and Bourne, P.E., 2000. The protein data bank. *Nucleic acids research*, *28*(1), pp.235-242.

De Arcangelis, L., Redner, S. and Coniglio, A., 1985. Anomalous voltage distribution of random resistor networks and a new model for the backbone at the percolation threshold. *Physical Review B*, *31*(7), p.4725.

Du, X., Li, Y., Xia, Y. L., Ai, S. M., Liang, J., Sang, P., Ji, X.-L. and Liu, S. Q., 2016. Insights into Protein–Ligand interactions: mechanisms, models, and methods. *International journal of molecular sciences*, *17*(2), pp.144-177.

Iliuk, A.B., Hu, L. and Tao, W.A., 2011. Aptamer in bioanalytical applications. *Analytical chemistry*. 83(12), pp. 4440-52.

Ellington, A.D. and Szostak, J.W., 1990. *In vitro* selection of RNA molecules that bind specific ligands. *Nature*, 346, pp.818–822.

Jo, H. and Ban, C., 2016. Aptamer–nanoparticle complexes as powerful diagnostic and therapeutic tools. *Experimental & Molecular Medicine*. 48(5). e230.

Kobilka, B.K. and Deupi, X., 2007. Conformational complexity of G-protein-coupled receptors. *Trends in pharmacological sciences*, *28*(8), pp.397-406.

Ni, X., Castanares, M., Mukherjee, A., Lupold, SE., 2011. Nucleic acid aptamers: clinical applications and promising new horizons. *Current medicinal chemistry*. *18(27),* p.4206.

Ohshiro, T., Matsubara, K., Tsutsui, M., Furuhashi, M., Taniguchi, M. and Kawai, T., 2012. Single-molecule electrical random resequencing of DNA and RNA. *Scientific reports*, *2*, p.501.

Oliphant, AR, Brandl, C.J. and Struhl, K., 1989. Defining the sequence specificity of DNA-binding proteins by selecting binding sites from random-sequence oligonucleotides: analysis of yeast GCN4 proteins. *Mol. Cell. Biol. 9*, pp. 2944–2949.

Onuchic, J.N., Luthey-Schulten, Z. and Wolynes, P.G., 1997. Theory of protein folding: the energy landscape perspective. *Annual review of physical chemistry*, *48*(1), pp.545-600.

Pennetta, C., Alfinito, E., Reggiani, L., Fantini, F., DeMunari, I. and Scorzoni, A., 2004. Biased resistor network model for electromigration failure and related phenomena in metallic lines. *Physical Review B*, *70*(17), p.174305.

Russo-Krauss, I., Merlino, A., Randazzo, A., Novellino, E., Mazzarella, L. and Sica, F.,2012. High-resolution structures of two complexes between thrombin and thrombin-binding aptamer shed light on the role of cations in the aptamer inhibitory activity. *Nucleic Acids Research. 40*, gks 512.

Schultze, P., Macaya, R.F. and Feigon, J., 1994. Three-dimension al solution structure of the thrombin-binding DNA aptamer d (GGTTGGTGTGGTTGG). *Journal of molecular biology*. 235, pp. 1532-1547.

Šponer, J., Leszczynski, J. and Hobza, P ., 2001. Electronic Properties, Hydrogen Bonding, Stacking,and Cation Binding of DNA and RNA Bases. *Nucleic Acid Sci*., *(61),* pp.3–31.

Sun, H., Zhu, X., Lu, P. Y., Rosato, R.R., Tan, W. and Zu, Y., 2014. Oligonucleotide aptamers: new tools for targeted cancer therapy*, Molecular Therapy-Nucleic Acids* 3, e182.

Tuerk, C. and Gold, L., 1990. Systematic evolution of ligands by exponential enrichment: RNA ligands to bacteriophage T4 DNA polymerase. *Science. 249*, pp.505–510.

Yüce M., Ullah N. and Budak H., 2015. Trends in aptamer selection methods and applications. *Analyst., 140(16)* , pp.5379-99